

Polaron lifetime and energy relaxation in semiconductor quantum dots

O. Verzele, R. Ferreira, and G. Bastard

Laboratoire de Physique de la Matière Condensée—Ecole Normale Supérieure, 24 rue Lhomond F-75005 Paris, France

(Received 5 May 2000)

We show that the anharmonicity driven instability of optical phonons leads in semiconductor quantum dots to a decay of polaron states which otherwise would be everlasting. By such a mechanism a single electron in an excited dot state can relax down to the ground state even if the electron energy difference markedly differs from the optical phonon energy.

Since early attempts^{1,2} to evaluate the electron energy-loss rate in semiconductor quantum dots, a number of papers have proposed various reasons why the predicted longitudinal-optical (LO) phonon bottleneck should be bypassed in actual dots (for phonon-related mechanisms see, e.g., Refs. 3–5 and for Auger effects see, e.g., Refs. 6–8). In particular, Li *et al.*⁵ have proposed that the finite LO phonon lifetime could alleviate the matching condition between the electron energy difference and the (quasimonochromatic) LO phonon energy which results from Fermi golden rule. Recent experiments⁹ and calculations^{9,10} have pointed out that electrons and optical phonons in quantum dots are in a strong-coupling regime. This implies that their coupling can never be accounted for perturbatively and that, in fact, electrons and phonons form mixed modes. These mixed modes, the polarons, would be everlasting⁹ if both their constituents, the electron and the phonons, were stable elementary excitations. The electron lifetime (limited by radiative decay in the case of photoexcitation of ideal dots) is long, typically 1 ns. Such is not the case of the LO phonons which are known in bulk semiconductors to disintegrate into two less energetic phonons due to the crystal anharmonicity (see, e.g., Ref. 11). The lifetime of LO phonons is 2 ps at room temperature in bulk GaAs.¹¹ Hence, in a semiconductor quantum dot, the polaron decay will be triggered by the instability of its phonon component. We stress in this work that in contrast to bulk or quantum-well structures the energy relaxation in quantum dots is not due to the processes involving the emission of *one* LO phonon but of *two* phonons and that the relaxation mechanism is not associated to the sole electron–LO phonon coupling but rather to the phonon-phonon interaction on polaron states. This implies, in particular, that there is no need for the two electron states to differ by one LO phonon energy because the energy conservation in this relaxation path is that of the polaron, which may greatly differ from the electron one due to the strong-coupling regime between electrons and LO phonons in quantum dots. This relaxation mechanism in quantum dots is assessed in the following.

We consider for simplicity the lower lying bound electron states in a nanometric quantum dot. To be specific we consider the case of InAs/GaAs dots. Their electron states can be approximately labeled by the z projection of the angular momentum of their envelope functions. Hereafter, they will be denoted $|S\rangle$ and $|P\pm\rangle$ with a typical energy distance of 50 meV.⁹ In quantum dots the electron–optical-phonon interac-

tions affect the electron states in drastically different ways. First, they give rise to polarons. The polaron states are the coherent superpositions of electrons and the particular combinations of LO phonon modes which diagonalize the electron-phonon interaction (here the Fröhlich Hamiltonian). These coherent admixtures produce interaction energies of several meV making the polarons very stable entities.⁹ However, the polarons are not everlasting because they are weakly perturbed by nonresonant interactions with the huge continuum of the other phonon modes (optical or acoustical), which lead to their damping.⁵ The lifetime broadening of the polaron states are of the order of 0.1 meV (see below), thus considerably smaller than the polaron energy coupling. It is then natural to start with an unperturbed basis which is that of the polaron and, in a second step, to study its relaxation through its coupling to a reservoir of phonon states. We note that the use of a density matrix for the polaron relaxation and not only that of a non-Hermitian Hamiltonian⁵ is necessary if one wants to study population transients, in particular, that of the ground state.¹² In addition, the knowledge of the polaron density matrix, in particular, its off diagonal elements, will give important insights on the possible use of quantum dot structures in the realization of long-lived entangled states.

Self-organized dots (say InAs) buried in a semiconductor matrix (say GaAs) have a nontrivial lens shape. More importantly, during the burying step of their fabrication their shape and composition are significantly altered compared to those of the naked dots.¹³ In particular, interdiffusion between the matrix and the host and strain inhomogeneities takes place, which affects their vibrational spectra. There is no detailed knowledge of the phonon spectra for actual self-organized dots. In the following, we shall use bulk phonons, i.e., labeled by a three-dimensional wave vector to identify the phonon eigenstates. This procedure has produced a good description of the polaron states observed in magneto-optical experiments⁹ and ultimately rests on the very large number of units cells enclosed in an actual InAs dot.

In the following we neglect the dot anisotropy, use effective-mass approximation with cylindrical symmetry to calculate the one particle states, and restrict our considerations to the lower-lying polaron states in which the number of phonons per mode is at most one and only the $|S\rangle$ and $|P\pm\rangle$ electronic states are included. If there are N optical modes labeled by their wave vectors \mathbf{Q}_i ($i=1, \dots, N$), the $N+3$ uncoupled states are therefore $|S0\rangle=|S\rangle\otimes|0\rangle$, $|P\pm 0\rangle=|P\pm\rangle\otimes|0\rangle$, $|S1\rangle=|S\rangle\otimes|1Q_i\rangle$. The diagonaliza-

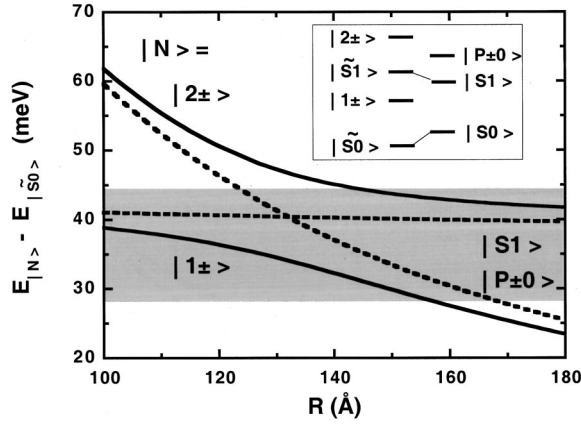


FIG. 1. Calculated R dependences of polaron energy differences $E_{|2\pm\rangle} - E_{|\tilde{S}0\rangle}$ and $E_{|1\pm\rangle} - E_{|\tilde{S}0\rangle}$ (solid lines) for truncated InAs cones with a fixed aspect ratio ($h/R=12/80$) floating on a 3.33-\AA InAs wetting layer. The shaded area represents the energy window where two-phonons relaxations for polarons are possible.

tion of the Fröhlich Hamiltonian within that basis produces $N-3$ linear superpositions of $|S\rangle \otimes |1Q_i\rangle$ states which are uncoupled to $|S0\rangle$ and $|P\pm\rangle$. These are basically LO phonon states uncoupled to the electrons, as witnessed by their insensitivity to the energy separation between $|S\rangle$ and $|P\pm\rangle$. Such is not the case of the remaining six polaron states whose wave functions have a nonzero projection on the basis states relevant to the electronic relaxation problem. They will be labeled $|\tilde{S}0\rangle$ (ground state), $|\tilde{S}1\rangle$, $|1\pm\rangle$, and $|2\pm\rangle$ (see inset of Fig. 1). The latter are twice degenerate on account of the $|P\pm\rangle$ degeneracy. Figure 1 shows for truncated cones (radius R , height h , with fixed aspect ratio $h/R=12/80$) the R dependence of the polaron energies measured from the ground polaron state, i.e., $E_{|1\pm\rangle} - E_{|\tilde{S}0\rangle}$ and $E_{|2\pm\rangle} - E_{|\tilde{S}0\rangle}$ (solid lines). We have used the material parameters deduced from magneto-optical data:⁹ a carrier effective mass of $0.067m_0$ and a dimensionless coupling constant between electrons and LO phonons $\alpha=0.15$. The LO phonon energies were taken dispersionless at $\hbar\omega_{\text{LO}}=36.4$ meV. For comparison, we have also plotted in Fig. 1 the R variations of the energies $E_{|P\pm\rangle}$ and $E_{|S\rangle} + \hbar\omega_{\text{LO}}$ (also measured from $E_{|\tilde{S}0\rangle}$; dotted lines). These noninteracting levels cross near $R=130$ Å. This crossing is replaced by a large anticrossing (12 meV), where the polaron wave functions display the maximum mixing between the unperturbed states.

Next, we consider the polaron as a small system interacting with a thermostat which comprises the acoustical and optical-phonon modes (but the six linear combinations are involved in the polaron states). At thermal equilibrium the thermostat imposes its temperature to the polaron. Through their mutual energy exchanges, it also governs the polaron relaxation if the latter is driven off equilibrium. The energy exchanges arise from the anharmonicity which converts one optical phonon into two less energetic phonons. In the following, we assume like in bulk GaAs (Ref. 11) that the emitted phonons are at the zone edge, one being acoustical (TA) while the other belongs to the optical modes. To keep a simple description of the anharmonicity we write the phonon-phonon Hamiltonian as

$$H_{\text{int}} = \sum_{\mathbf{Q}, \mathbf{k}_1, \mathbf{k}_2} W(\mathbf{Q}) a_{\mathbf{Q}} a_{\mathbf{k}_1}^\dagger c_{\mathbf{k}_2}^\dagger + (\text{H.c.}), \quad (1)$$

where $a_{\mathbf{Q}}$ ($a_{\mathbf{Q}}^\dagger$) is the destruction (creation) operator of one LO phonon with wave vector \mathbf{Q} while $c_{\mathbf{k}_2}^\dagger$ is the creation operator of the emitted acoustical phonon. H_{int} is also the Hamiltonian which couples the polaron to the reservoir through its LO phonon component. In bulk materials H_{int} leads to a finite lifetime of LO phonons.¹¹ By using the Fermi golden rule, one gets the energy conservation $E(\mathbf{Q}) = E(\mathbf{k}_1) + E(\mathbf{k}_2)$. In addition, the crystal translation invariance restricts the available \mathbf{k} 's since $W(\mathbf{Q})$ is nonzero only if $\mathbf{Q} = \mathbf{k}_1 + \mathbf{k}_2$. We shall thus employ the Fermi golden rule to evaluate the effects of H_{int} on the mixed states $|p_i\rangle \otimes |t_j\rangle$, where $|p_i\rangle$ and $|t_j\rangle$ are the polaron and two-phonons thermostat states, respectively. In addition, since the only LO modes which are effectively coupled to the electron in the polaron states have small \mathbf{Q} ,⁹ we shall neglect the \mathbf{Q} dependence of $W(\mathbf{Q})$, i.e., set $W(\mathbf{Q}) = W_0$, where W_0 is an effective coupling strength between the polaron and the reservoir. This strength is fixed by requiring the lifetime of a LO phonon with $\mathbf{Q}=\mathbf{0}$ in a bulk material to be 2 ps at room temperature¹¹ (ensuring the wave-vector conservation during the phonon decay). In the calculations the phonon density of states repeatedly appears. We have used a rounded off bulk one, which results from isotropic phonon dispersions taken as two matching pieces of parabolas extending from 28 to 36.4 meV for the LO phonons and a linear segment matching a piece of parabola for the transverse-acoustical branch extending from 0 to 8 meV. This implies that the thermostat (two-phonon) continuum has a finite width for the relaxation mechanisms we consider since it extends from 28 to 44.4 meV (shaded area in Fig. 1).

The diagonal elements of the polaron density matrix, the populations f_n , are known¹² to fulfill rate equations of the form

$$df_n/dt = \sum_m \{-f_n \Gamma_{n \rightarrow m} + f_m \Gamma_{m \rightarrow n}\} \quad (2a)$$

$$\Gamma_{m \rightarrow n} = (2\pi/\hbar) \sum_{\mu} p_{\mu} \sum_{\nu} |\langle t_{\nu}, m | H_{\text{int}} | t_{\mu}, n \rangle|^2 \times \delta[E_n - E_m + E_{\mu} - E_{\nu}] \quad (2b)$$

with $|t_{\mu}\rangle$ and $|t_{\nu}\rangle$ being thermostat states distributed according to the equilibrium distribution function p_{μ} . Since the coupling to the thermostat involves only phonon operators, the polaron states, $|1\pm\rangle$, $|2\pm\rangle$, and $|\tilde{S}1\rangle$ have a direct coupling only to $|\tilde{S}0\rangle$. In principle, $|2\pm\rangle$ could be coupled to $|\tilde{S}1\rangle$ but for the R values considered here this coupling vanishes because the energy difference between these two states is too small. Figure 2 shows the calculated temperature dependences of $\Gamma_{|1\pm\rangle}$ for the relaxation along the path $|1\pm\rangle \rightarrow |\tilde{S}0\rangle$ for several values of the dot radius R . This path is very efficient at small R (~ 0.25 ps⁻¹ at low T) where the initial state resembles unperturbed $|S1\rangle$ states (see Fig. 1). It

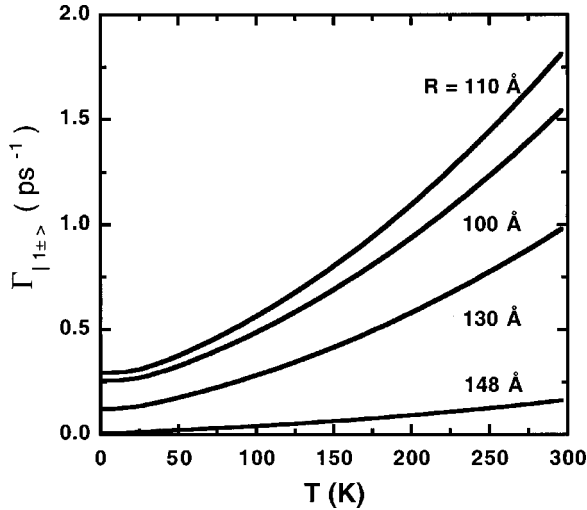


FIG. 2. Calculated temperature dependence of the decay rate $\Gamma_{|1\pm\rangle}$ for the population of the polaron level $|1\pm\rangle$ for several values of the dot radius R of truncated InAs dots floating on a 3.33-Å InAs wetting layer with a fixed aspect ratio ($h/R=12/80$).

is almost constant with increasing R up to ~ 125 Å to finally become forbidden at $R > 158$ Å because of the unavailability of two-phonon thermostat states which could match an energy difference between polaron states smaller than 28 meV. The relaxation rates increase with increasing temperature because they involve $(1+n_{k1})(1+n_{k2})$. However, no clear T^2 or T dependence is obtained because kT is never very large compared to all the phonon energies. As for the relaxation along the path $|2\pm\rangle \rightarrow |\widetilde{S0}\rangle$ (not shown) we find it forbidden at small R ($R < 146$ Å) because the separation of the $|2\pm\rangle$ and $|\widetilde{S0}\rangle$ levels is larger than the topmost two phonon thermostat energy (see Fig. 1). For larger R , the relaxation is fast but this is because the $|2\pm\rangle$ level resembles more and more the $|S1\rangle$ states (see Fig. 1).

It is instructive to compare this phenomenological but microscopic model to the “semiclassical” predictions. In the latter description, the polaron decay rate is equal to the bulk LO phonon decay rate times the probability to find one phonon in the polaron state. With such a model there is no energy window outside which the polaron relaxation is impossible. Rather, the polaron semiclassical decay rate decreases monotonously for polaron states which are more and more detuned from the resonance condition. A comparison between the calculated R dependence of the polaron decay rates in both the microscopic and “semiclassical” (not shown) shows a relatively good agreement at large detunings (say a factor of 2 between the two rates) but the semiclassical picture becomes grossly inaccurate when the polaron should release an energy outside the energy window.

Figure 3(a) shows the population evolution of the polaron states at $T=300$ K in the case $R=160$ Å. The initial condition was that both $|2\pm\rangle$ levels were equally populated at $t=0$, i.e., $f_{|2+\rangle}(t=0)=f_{|2-\rangle}(t=0)=1/2$ while $f_i(t=0)=0$ if $i \neq |2\pm\rangle$. The populations shown in Fig. 3(a) include the twofold degeneracy of $|2\pm\rangle$. The levels $|\widetilde{S0}\rangle$ are never populated because they are too close from $|\widetilde{S0}\rangle$ and $|2\pm\rangle$. One sees that the characteristic time constant to reach ther-

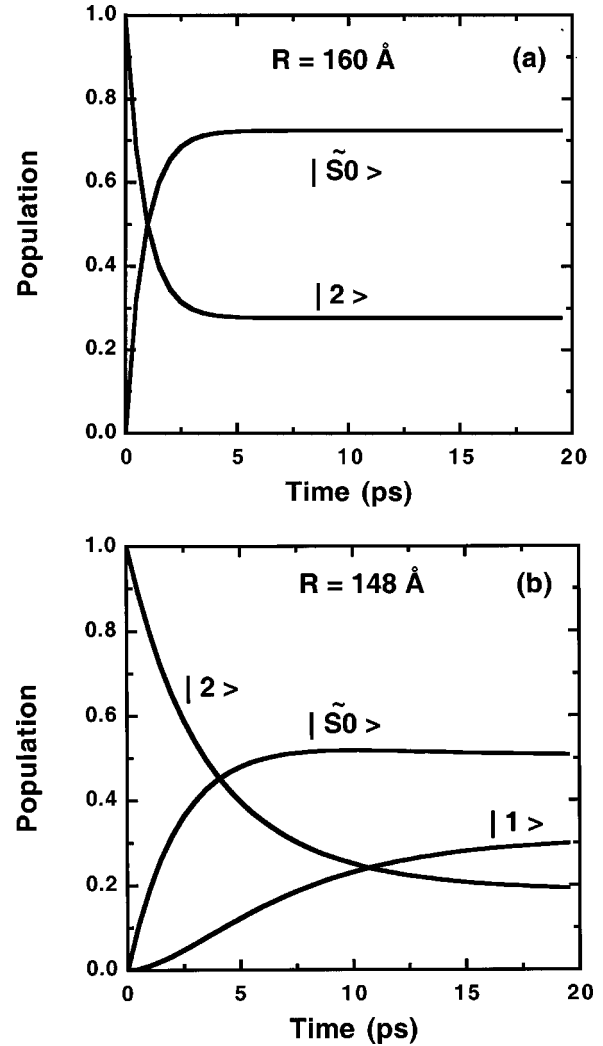


FIG. 3. (a) Calculated time dependences of the polaron populations at $T=300$ K for truncated InAs cones with $R=160$ Å and $h=24$ Å floating on a 3.33-Å InAs wetting layer. (b) Same as (a), but for $R=148$ Å and $h=22.2$ Å.

mal equilibrium is very short (~ 3 ps). These times are upper limits for the decoherence time of the polaron states. Figure 3(b) shows a similar plot for $R=148$ Å where both $|1\pm\rangle$ and $|2\pm\rangle$ are coupled to $|\widetilde{S0}\rangle$, although the relaxation time from $|2\pm\rangle$ to $|\widetilde{S0}\rangle$ is long (21.2 ps). Although the relaxation of the various populations to their thermodynamical equilibrium values cannot be fitted by single exponentials, one can define characteristic time constants as the time required to reach halfway of the equilibrium value for the different populations. We find ~ 7 ps for $f_{|1\pm\rangle}$ and ~ 2.5 ps for both $f_{|2\pm\rangle}$ and $f_{|\widetilde{S0}\rangle}$.

In the secular approximation, the off-diagonal terms of the polaron density matrix, the coherences σ_{nm} , display damped oscillations:

$$\sigma_{nm}(t) = \sigma_{nm}(0) \exp\{-t(\Gamma_{nm} + i\Omega_{nm})\}, \quad (3a)$$

$$\Gamma_{nm} = (\Gamma_n + \Gamma_m)/2; \quad \hbar\Omega_{nm} = E_n - E_m. \quad (3b)$$

At room temperature, for instance, we find $1/\Gamma_{|1\pm\rangle,|2\pm\rangle} = 2.3$ ps for $R=160$ Å while for $R=148$ Å, we find $1/\Gamma_{|1\pm\rangle,|2\pm\rangle} = 5$ ps.

The LPMC-ENS is Unité Associée au CNRS (UMR 8551) et aux Universités Paris 6 et Paris 7. This work was

partly supported by a New Energy and Industrial Technology Development Organization (NEDO) grant and by a E.E.C. Project No. IST-1999-11311 (SQID). We thank J. M. Gérard, Y. Guldner, P. Petroff, and H. Sakaki for useful discussions.

¹U. Bockelmann and G. Bastard, Phys. Rev. B **42**, 8947 (1990).

²H. Benisty, C. M. Sottomayor-Torres, and C. Weisbuch, Phys. Rev. B **44**, 10 945 (1991).

³T. Inoshita and H. Sakaki, Phys. Rev. B **46**, 7260 (1992).

⁴D. F. Schroeter, D. J. Griffiths, and P. C. Sercel, Phys. Rev. B **54**, 1486 (1996).

⁵X. Q. Li, H. Nakayama, and Y. Arakawa, Phys. Rev. B **59**, 5069 (1999).

⁶A. V. Uskov, J. McInemey, F. Adler, H. Schweitzer, and M. H. Pilkuhn, Appl. Phys. Lett. **72**, 58 (1998).

⁷U. Bockelmann and T. Egeler, Phys. Rev. B **46**, 15 574 (1992).

⁸R. Ferreira and G. Bastard, Appl. Phys. Lett. **74**, 2818 (1999).

⁹S. Hameau, Y. Guldner, O. Verzelen, R. Ferreira, G. Bastard, J. Zeman, A. Lemaitre, and J. M. Gérard, Phys. Rev. Lett. **83**, 4152 (1999).

¹⁰T. Inoshita and H. Sakaki, Phys. Rev. B **56**, R4355 (1997).

¹¹F. Vallée and F. Bogani, Phys. Rev. B **43**, 12 049 (1991). See also F. Vallée, *ibid.* **49**, 2460 (1994).

¹²C. Cohen-Tannoudji, J. Dupont-Roc, and G. Grynberg, *Processus d'interaction Entre Photons et Atomes* (InterEditions/Editions du CNRS, Paris, 1988).

¹³P. W. Fry *et al.*, Phys. Rev. Lett. **84**, 733 (2000).